International Journal of GEOMATE, July 2023, Vol. 25, Issue 107, pp.123-132
ISSN: 2186-2982 (P), 2186-2990 (O), Japan, DOI: https://doi.org/10.21660/2023.107.3830
Geotechnique, Construction Materials and Environment

APPLICATION OF A FRACTIONAL STEP ALGORITHM FOR THE THREE-DIMENSIONAL SHALLOW WATER EQUATIONS IN A ROTATING SPHERICAL SURFACE

*Medhat Helal[1]

[1]Civil Engineering Department, College of Engineering and Islamic Architecture, Umm Al-Qura University, Makkah, Saudi Arabia, Department of Engineering Mathematics and Physics, Zagazig University, Zagazig, Egypt

*Corresponding Author, Received: 21 Feb. 2023, Revised: 26 March 2023, Accepted: 02 April 2023

ABSTRACT: This paper is mainly concerned with the motion of an incompressible fluid in a slowly rotating spherical basin using the fractional step method. The algorithm is applied by splitting the three-dimensional shallow water equations into three problems each of one dimension in every direction using the Riemann invariant. The next step is the successive integration in all directions along the characteristics associated with cubic spline interpolation. It has the advantage of reducing the three-dimensional matrix problem into an equivalent one-dimensional problem, the simplicity of this algorithm makes it very suitable for parallel computers. Numerical results are represented in three-dimensional for the velocity components at different times with different Coriolis parameters. It is worthy to note that such a study has useful applications in the science of oceanography.

Keywords: Rotating spherical surface, Shallow water equations, Fractional step method, Riemann invariants, cubic spline interpolation

1. INTRODUCTION

Recently, the problem of solving the shallow water equations on a sphere has attracted growing interest. As one might expect, the fluid mechanics of rotating flows is more fully developed in the field of geophysics than it is in the field of aerodynamics. Rotating fluids in spherical basins simulate many natural free surface flow problems like those of closed seas and lakes. In astrophysical and geophysical fluids, rotation is often playing a main part. In these common cases, the Coriolis force is the dominant force and so it must be included in the mathematical model.

The numerical treatment for nonlinear systems descriptive of fluid motions was firstly given by Rayleigh [1] in 1903 who investigated the vibrations of a rectangular sheets of rotating liquid. Greenspan in 1968 [2] gave a detailed and excellent study of rotating fluids in his famous book. A uniform flow on an open channel is studied in [3], shallow water equations are used as the model by involving the bottom topography. The Nonlinear shallow water Equation [4] has been applied as the fundamental model. The equation has been solved analytically and numerically to obtain the run-up coefficient.

The object of this work is to find a complete study of the wave motion through the evaluation of the wave height and velocity components for the rotating liquid inside a spherical basin and suggests a mathematical treatment depending on the application of a fractional step method. This method has the great advantage of solving the shallow water equations without iterative steps involved in the multidimensional interpolation problems. The absence of iterative steps in this technique makes it very suitable for problems in which small time steps and grid sizes are required. It has been pointed out some time ago by Yakimiw and Robert [5] in 1986, that the method of fractional step for the numerical solution of the shallow water equations has also the advantage of reducing the multidimensional matrix inversion problem into an equivalent one-dimensional problem, so the technique becomes very simple and very attractive to apply. It has also the great advantage of solving the shallow water equations without the iterative steps involved in the multidimensional interpolation problems so that it reduces the numerical diffusion and makes it suitable for problems in which small time steps and grid sizes are required. In the present paper, we apply this technique by splitting the shallow water equations and successively integrating in every direction along the characteristics of the Riemann invariants associated with cubic spline interpolation, see Shoucri [6] and [7] who applied the fractional step method for the numerical solution of the shallow water equations in their simplest form. In 1980, Simulating Wave Near-shore [8] is a numerical wave model for hindcasting or forecasting wave parameters in coastal areas. This numerical model is chosen because is suitable for shallow water.

In this paper, we used the fractional step approach to study the motion of an incompressible fluid in a spherically rotating basin. The Riemann invariant is used to divide the three-dimensional shallow water equations into three one-dimensional problems, each with one dimension in every direction. The subsequent step is the next integration along the properties related to cubic spline interpolation in all directions. The numerical results are shown for the velocity components at various times and for various Coriolis values.

2. RESEARCH SIGNIFICANCE

For the numerical solution of the three-dimensional nonlinear shallow water problem, we use the fractional step approach. By employing the Riemann invariants, the three-dimensional shallow water equations are divided into three one-dimensional problems. The method is the best one for parallel architecture computers since it is so straightforward. Since the approach generates the equations without the iterative steps necessary to solve the multidimensional interpolation problem, it is effective and has less numerical diffusion. Without any computer issues and without requiring a lot of RAM, we may reduce the time steps and grid size to boost accuracy.

3. SHALLOW WATER EQUATIONS ON A SPHERE

on the surface of the rotating sphere which has a domain occupied by the liquid as

$$0 \le z \le h, \qquad -R \le x, y \le R \tag{1}$$

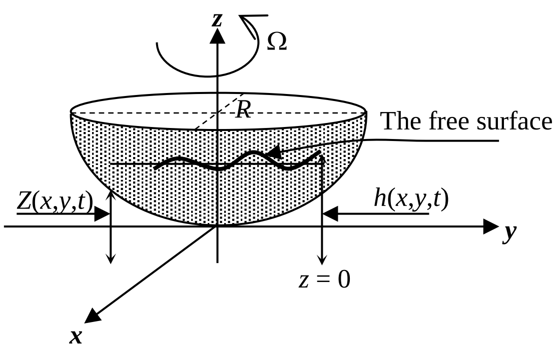

Fig.1 Geometry of a rotating sphere with a shallow liquid

The relevant hydrodynamic equations consist of the
continuity equation

$$u_x + \upsilon_y + w_z = 0\,, \tag{2}$$

together with the equations of motion

$$u_t + uu_x + \upsilon u_y + wu_z - f\,\upsilon + \frac{1}{\rho}\,p_x = 0\,, \tag{3}$$

$$\upsilon_t + u\upsilon_x + \upsilon\upsilon_y + w\upsilon_z + f\,u + \frac{1}{\rho}\,p_y = 0\,, \tag{4}$$

$$w_t + uw_x + \upsilon w_y + ww_z + g + \frac{1}{\rho}\,p_z = 0\,, \tag{5}$$

where, in the usual notation, f is the Coriolis parameter being the rotation rate of the sphere and equal to the angular speed of the system (f = 2Ω), "u", "υ" and "w" are the components of the velocity in the three Cartesian directions (x, y, z). The shallow water equations model the propagation of disturbances in water and other incompressible fluids [9]. The incompressible fluid has density ρ and pressure p the first is assumed constant; g denotes the acceleration due to gravity.

The flow is bounded below by the surface of the spherical basin $z = Z(x, y)$ and above by the free surface $z = h(x, y, t)$. The boundary conditions, therefore, are

i) At the lower boundary $z = Z(x, y)$:

$$uZ_x + \upsilon Z_y = w, \qquad \text{on } z = Z(x, y)\,. \tag{6}$$

ii) On the free surface $z = h(x, y, t)$:

$$h_t + uh_x + \upsilon h_y = w \qquad \text{on } z = h(x, y, t) \tag{7}$$

The initial conditions are $u = \upsilon = w = 0$.

Also, on the free surface $z = h(x, y, t)$, the pressure is assumed to be constant on the free surface, equal to p_0, say. The hydrostatic pressure p is replaced by the uniform gravitational pressure

$$p = p_0 + \rho g(h - z)\,, \tag{8}$$

Elimination of p from (3)-(5), with the help of (8), therefore the governing equations of motion become

$$u_t + uu_x + \upsilon u_y + wu_z - f\,\upsilon + gh_x = 0\,, \tag{9}$$

$$\upsilon_t + u\upsilon_x + \upsilon\upsilon_y + w\upsilon_z + f\,u + gh_y = 0\,, \tag{10}$$

$$w_t + uw_x + \upsilon w_y + ww_z = 0\,. \tag{11}$$

For convenience, we recast the system of governing equations and auxiliary conditions into a simplified form. Redefining the variables as follows:

$$\zeta = \frac{z}{h}\,, \quad \bar{\zeta} = \frac{Z}{h}\,, \quad \omega = \frac{1}{h}\Big(w - \zeta(h_t + uh_x + \upsilon h_y)\Big), \tag{12}$$

Introducing these new variables into the continuity equation (2) and the equations of motion (9)-(11) to obtain the problem in the form:

$$
\begin{aligned}
&h_t + (uh)_x + (\upsilon h)_y + (\omega h)_\zeta = 0\\
&(uh)_t + (u^2 h + \tfrac{1}{2} g h^2)_x + (u\upsilon h)_y + (u\omega h)_\zeta = hf\upsilon\\
&(\upsilon h)_t + (u\upsilon h)_x + (\upsilon^2 h + \tfrac{1}{2} g h^2)_y + (\upsilon\omega h)_\zeta = -hf\,u\\
&(\omega h)_t + (u\omega h)_x + (\upsilon\omega h)_y + (\omega^2 h)_\zeta = 0
\end{aligned}
\tag{13}
$$

The shallow water equations can be embedded in the system.

$$\frac{\partial \mathrm{v}_s}{\partial t} + S(\mathrm{v}_s)\mathrm{v}_s + \alpha + \beta + \gamma = 0\,, \tag{14}$$

where $\mathrm{v}_s = (u,\, \upsilon,\, w,\, h)^T$ and $\mathrm{v}_s =$

$$
\begin{pmatrix}
\dfrac{\partial u}{\partial r} & \dfrac{1}{r}\dfrac{\partial u}{\partial \theta} & \dfrac{1}{r\cos\theta}\left(\dfrac{\partial u}{\partial \lambda} - \upsilon\sin\theta + w\cos\theta\right)\\
\dfrac{\partial \upsilon}{\partial r} & \dfrac{1}{r}\left(\dfrac{\partial \upsilon}{\partial \theta} + w\right) & \dfrac{1}{r\cos\theta}\left(\dfrac{\partial \upsilon}{\partial \lambda} - u\sin\theta\right)\\
\dfrac{\partial w}{\partial r} & \dfrac{1}{r}\left(\dfrac{\partial w}{\partial \theta} - \upsilon\right) & \dfrac{1}{r\cos\theta}\left(\dfrac{\partial w}{\partial \lambda} - u\cos\theta\right)\\
\dfrac{1}{r\cos\theta}\dfrac{\partial h}{\partial \lambda} & \dfrac{1}{r}\left(\dfrac{\partial h}{\partial \theta} + h\tan\theta\right) & 0
\end{pmatrix}
\tag{15}
$$

$$\alpha = \begin{pmatrix} 0\\ 0\\ \dfrac{u^2+\upsilon^2}{2}\\ 0 \end{pmatrix}, \tag{16}$$

$$\beta = \begin{pmatrix} \dfrac{g}{r\cos\theta}\dfrac{\partial h}{\partial \lambda}\\ \dfrac{g}{r}\dfrac{\partial h}{\partial \theta}\\ 0\\ \dfrac{h}{r\cos\theta}\left(\dfrac{\partial u}{\partial \lambda} + \dfrac{\partial \upsilon}{\partial \theta}\cos\theta\right) \end{pmatrix}, \tag{17}$$

and

$$\gamma = \begin{pmatrix} -f\upsilon\\ f\,u\\ 0\\ 0 \end{pmatrix}, \tag{18}$$

$$\frac{\partial h}{\partial t} + \frac{u}{r\cos\theta}\frac{\partial h}{\partial \lambda} + \frac{\upsilon}{r}\frac{\partial h}{\partial \theta} + \frac{h}{r\cos\theta}\frac{\partial u}{\partial \lambda} + \frac{h}{r\cos\theta}\frac{\partial(\upsilon\cos\theta)}{\partial \theta} = 0$$

$$\frac{\partial u}{\partial t} + w\frac{\partial u}{\partial r} + \frac{u}{r\cos\theta}\frac{\partial u}{\partial \lambda} + \frac{\upsilon}{r}\frac{\partial u}{\partial \theta} + \frac{g}{r\cos\theta}\frac{\partial h}{\partial \lambda} = \frac{u\upsilon\tan\theta}{r} - \frac{uw}{r} + f\upsilon$$

$$\frac{\partial \upsilon}{\partial t} + w\frac{\partial \upsilon}{\partial r} + \frac{u}{r\cos\theta}\frac{\partial \upsilon}{\partial \lambda} + \frac{\upsilon}{r}\frac{\partial \upsilon}{\partial \theta} + \frac{g}{r}\frac{\partial h}{\partial \theta}(+w) = -\frac{u^2\tan\theta}{r} - \frac{\upsilon w}{r} - f\,u$$

$$\frac{\partial w}{\partial t} + w\frac{\partial w}{\partial r} + \frac{\upsilon}{r}\frac{\partial w}{\partial \theta} + \frac{u}{r\cos\theta}\frac{\partial w}{\partial \lambda} = 0$$

the boundary conditions (6) and (7) simplify to

$$-\bar{\zeta} h_t + u\bar{\zeta}_x + \upsilon\bar{\zeta}_y = \omega \qquad \text{on } \zeta = \bar{\zeta} \tag{19}$$

$$\omega = 0 \qquad \text{on } \zeta = 1\,. \tag{20}$$

4. METHOD OF FRACTIONAL STEP

Systems of three-dimensional hyperbolic equations are sometimes split into a series of one-dimensional operators known as fractional steps, see Yanenko [10]. We depend on Strang's fractional step method [11,12] which is more accurate in time where it has a second-order accurate but not on Godunov's fractional step method [13] which in the first order accurate in time. The fractional step technique is applied to equations (13), to advance the equation by a time step, as follows:

Step 1. Solve for $\Delta t/2$ in the r direction:

$$
\begin{aligned}
&h_t + (uh)_x = 0,\\
&(uh)_t + (u^2 h + \tfrac{1}{2} g h^2)_x = 0,\\
&(\upsilon h)_t + (u\upsilon h)_x = 0,\\
&(\omega h)_t + (u\omega h)_x = 0.
\end{aligned}
\tag{21}
$$

The above equations reduce to

$$
\begin{aligned}
&\frac{\partial h}{\partial t} + u\frac{\partial h}{\partial x} + h\frac{\partial u}{\partial x} = 0,\\
&\frac{\partial u}{\partial t} + g\frac{\partial h}{\partial x} + u\frac{\partial u}{\partial x} = 0,\\
&\frac{\partial \upsilon}{\partial t} + u\frac{\partial \upsilon}{\partial x} = 0,\\
&\frac{\partial \omega}{\partial t} + u\frac{\partial \omega}{\partial x} = 0.
\end{aligned}
\tag{22}
$$

Equations (22) can be rewritten as

$$
\begin{aligned}
&\frac{\partial R_{x\pm}}{\partial t} + (u \pm \sqrt{gh})\frac{\partial R_{x\pm}}{\partial x} = 0,\\
&\frac{\partial \upsilon}{\partial t} + u\frac{\partial \upsilon}{\partial x} = 0,\\
&\frac{\partial \omega}{\partial t} + u\frac{\partial \omega}{\partial x} = 0,
\end{aligned}
\tag{23}
$$

where $R_{x\pm} = u \pm 2\sqrt{gh}$ is the Riemann invariant. We apply the classical finite difference scheme to Eqs. (23), for example, the first row of Eqs. (23) in the positive direction becomes:

$$\frac{R_{x+}(x,y,\zeta,t+\Delta t/2)-R_{x+}(x,y,\zeta,t)}{\Delta t/2} + \left(u(x,y,t)+\sqrt{gh(x,y,\zeta,t)}\right) \frac{R_{x+}(x,y,\zeta,t)-R_{x+}(x-\Delta x,y,\zeta,t)}{\Delta x}=0,$$

let $\frac{2\Delta x}{\Delta t}=u+\sqrt{gh}$, then the above equation reduces to:

$$R_{x+}\left(x,y,\zeta,t+\Delta t/2\right) = R_{x+}\left(x-(u+\sqrt{gh})\Delta t/2, y,\zeta,t\right).$$

Therefore, the solutions of Eqs. (23) for any value of y and ζ at $t+\Delta t/2$ is

$$R_{x\pm}\left(x,y,\zeta,t+\Delta t/2\right)=R_{x\pm}\left(x_{\pm},y,\zeta,t\right), \quad (24)$$

where $x_{\pm}=x-\left(u\pm\sqrt{gh}\right)\Delta t/2$.

Equation (24) means that the value $R_{x\pm}$ after the time $\Delta t/2$ from time t is the same value of $R_{x\pm}$ at the time t but after the distance x is shifted by $\left(u\pm\sqrt{gh}\right)\Delta t/2$. The shifted values are calculated from the values of the function at the grid points using a cubic spline interpolation. We use a simple cubic spline defined over three grid points, calculated by writing the function, and its first and second derivatives are continuous at the grid points. Details have been given in [14]. Testing this cubic spline polynomial against other methods [15] has shown that this cubic polynomial has low numerical diffusion compared to other polynomials, and;

$$\upsilon\left(x,\ y,\ \zeta,\ t+\Delta t/2\right)=\upsilon\left(x-u\frac{\Delta t}{2},\ y,\ \zeta,\ t\right), \quad (25)$$

Also,

$$\omega\left(x,\ y,\ \zeta,\ t+\Delta t/2\right)=\omega\left(x-u\frac{\Delta t}{2},\ y,\ \zeta,\ t\right), \quad (26)$$

i.e., the solution of the problem in system (22) at the end of the time $(n+1/2)\Delta t,\quad n=0,1,2,3,...$ reduces to the equality

$$\begin{pmatrix} R_{x\pm} \\ \upsilon \\ \omega \end{pmatrix}_{(x,\ y,\zeta,(n+1/2)\Delta t)} = \begin{pmatrix} R_{x\pm} \\ \upsilon \\ \omega \end{pmatrix}_{(x_{\pm},\ y,\zeta,n\Delta t)},$$

where $x_{\pm}=x-\left(u\pm\sqrt{gh}\right)\Delta t/2$ for the first row and $x_{\pm}=x-u\,\Delta t/2$ for the other rows.

Step 2. Solve for $\Delta t/2$ in the y direction:

$$\begin{aligned} &h_t+(\upsilon h)_y=0,\\ &(\upsilon h)_t+(\upsilon^2 h+\tfrac{1}{2}gh^2)_y=0,\\ &(uh)_t+(u\upsilon h)_y=0,\\ &(\omega h)_t+(\upsilon\omega h)_y=0. \end{aligned} \quad (27)$$

It is convenient to simplify the above equations to the form,

$$\begin{aligned} &\frac{\partial h}{\partial t}+\upsilon\frac{\partial h}{\partial y}+h\frac{\partial \upsilon}{\partial y}=0,\\ &\frac{\partial \upsilon}{\partial t}+g\frac{\partial h}{\partial y}+\upsilon\frac{\partial \upsilon}{\partial y}=0,\\ &\frac{\partial u}{\partial t}+\upsilon\frac{\partial u}{\partial y}=0,\\ &\frac{\partial \omega}{\partial t}+\upsilon\frac{\partial \omega}{\partial y}=0. \end{aligned} \quad (28)$$

Equation (28) is rewritten as

$$\begin{aligned} &\frac{\partial R_{y\pm}}{\partial t}+(\upsilon\pm\sqrt{gh})\frac{\partial R_{y\pm}}{\partial y}=0,\\ &\frac{\partial u}{\partial t}+\upsilon\frac{\partial u}{\partial y}=0,\\ &\frac{\partial \omega}{\partial t}+\upsilon\frac{\partial \omega}{\partial y}=0, \end{aligned} \quad (29)$$

where $R_{x\pm}=\upsilon\pm 2\sqrt{gh}$ is the Riemann invariant. The solutions of Eq. (29) for any value of x and ζ at $t+\Delta t/2$ is

$$R_{y\pm}\left(x,\ y,\ \zeta,\ t+\Delta t/2\right)=R_{y\pm}\left(x,\ y_{\pm},\ \zeta,\ t\right), \quad (30)$$

where $y_{\pm}=y-\left(\upsilon\pm\sqrt{gh}\right)\Delta t/2$, and,

$$u\left(x,\ y,\ \zeta,\ t+\Delta t/2\right)=u\left(x,\ y-\upsilon\frac{\Delta t}{2},\ \zeta,\ t\right), \quad (31)$$

Also,

$$\omega\left(x,\ y,\ \zeta,\ t+\Delta t/2\right)=\omega\left(x,\ y-\upsilon\frac{\Delta t}{2},\ \zeta,\ t\right). \quad (32)$$

Again, after the end of time $(n+1/2)\Delta t$, $n=0,1,2,3,...$ we find,

$$\begin{pmatrix} R_{y\pm} \\ u \\ \omega \end{pmatrix}_{(x,\ y,\zeta,(n+1/2)\Delta t)} = \begin{pmatrix} R_{y\pm} \\ u \\ \omega \end{pmatrix}_{(x,\ y_{\pm},\zeta,\ n\Delta t)},$$

where $y_{\pm} = y - \left(\upsilon \pm \sqrt{gh}\right)\Delta t/2$ for the first row and $y_{\pm} = y - \upsilon\,\Delta t/2$ for the other rows.

Step 3. Solve for $\Delta t/2$ in the ζ direction:

$$\begin{aligned} &h_t + (\omega h)_\zeta = 0,\\ &(uh)_t + (u\omega h)_\zeta = 0,\\ &(\upsilon h)_t + (\upsilon\omega h)_\zeta = 0,\\ &(\omega h)_t + (\omega^2 h)_\zeta = 0. \end{aligned} \tag{33}$$

Equations (33) are rewritten as

$$\begin{aligned} &\frac{\partial h}{\partial t} + h\frac{\partial \omega}{\partial \zeta} = 0,\\ &\frac{\partial u}{\partial t} + \omega\frac{\partial u}{\partial \zeta} = 0,\\ &\frac{\partial \upsilon}{\partial t} + \omega\frac{\partial \upsilon}{\partial \zeta} = 0,\\ &\frac{\partial \omega}{\partial t} + \omega\frac{\partial \omega}{\partial \zeta} = 0. \end{aligned} \tag{34}$$

The solutions of Eq. (34) for any value of y at $t + \Delta t/2$ is

$$\begin{aligned} h\left(x,\ y,\ \zeta,\ t + \Delta t/2\right) &= h\left(x,\ y,\ \zeta,\ t\right)\\ &\quad - \omega\left(x,\ y,\ \zeta,\ t\right) + \omega\left(x,\ y,\ \zeta - h\frac{\Delta t}{2},\ t\right) \end{aligned} \tag{35}$$

$$u\left(x,\ y,\ \zeta,\ t + \Delta t/2\right) = u\left(x,\ y,\ \zeta - \omega\frac{\Delta t}{2},\ t\right) \tag{36}$$

$$\upsilon\left(x,\ y,\ \zeta,\ t + \Delta t/2\right) = \upsilon\left(x,\ y,\ \zeta - \omega\frac{\Delta t}{2},\ t\right) \tag{37}$$

and;

$$\omega\left(x,\ y,\ \zeta,\ t + \Delta t/2\right) = \omega\left(x,\ y,\ \zeta - \omega\frac{\Delta t}{2},\ t\right). \tag{38}$$

Thirdly, after the end of time $(n+1/2)\Delta t$, $n = 0,1,2,3,...$ we find,

$$\begin{pmatrix} h\\ u\\ \upsilon\\ \omega \end{pmatrix}_{(x,\ y,\zeta,(n+1/2)\Delta t)} = \begin{pmatrix} h\\ u\\ \upsilon\\ \omega \end{pmatrix}_{(x,\ y,\zeta_-,\ n\Delta t)} + \begin{pmatrix} h-\omega\\ 0\\ 0\\ 0 \end{pmatrix}_{(x,\ y,\zeta,\ n\Delta t)}$$

where $\zeta_- = \zeta - h\ \Delta t/2$ for the first row and $\zeta_- = \zeta - \omega\ \Delta t/2$ for the other rows.

Step 4. Solve for the source term for Δt:

$$\frac{\partial u}{\partial t} = f\upsilon, \qquad \frac{\partial \upsilon}{\partial t} = -f\,u. \tag{39}$$

The solution of Equation (39) is calculated as

$$u\left(x,y,\zeta,t+\Delta t\right) = u\left(x,y,\zeta,t\right) + \Delta t\left\{ f\,\upsilon(x,y,\zeta,t)\right\}, \tag{40}$$

and;

$$\upsilon\left(x,y,\zeta,t+\Delta t\right) = \upsilon\left(x,y,\zeta,t\right) + \Delta t\left\{-f\,u(x,y,\zeta,t)\right\} \tag{41}$$

or calculated at $(n+1)\Delta t$, $n = 0,1,2,3,...$ we get,

$$\begin{pmatrix} u\\ \upsilon \end{pmatrix}_{(x,\ y,\zeta,(n+1)\Delta t)} = \begin{pmatrix} u + \Delta t\ f\,\upsilon\\ \upsilon - \Delta t\ f\,u \end{pmatrix}_{(x,\ y,\zeta,\ n\Delta t)},$$

Step 5. Apply the following equality in the ζ direction at time $(n+1)\Delta t$

$$\begin{pmatrix} h\\ u\\ \upsilon\\ \omega \end{pmatrix}_{(x,\ y,\zeta,(n+1)\Delta t)} = \begin{pmatrix} h\\ u\\ \upsilon\\ \omega \end{pmatrix}_{(x,\ y,\zeta_-,\ (n+1/2)\Delta t)} + \begin{pmatrix} h-\omega\\ 0\\ 0\\ 0 \end{pmatrix}_{(x,\ y,\zeta_-,\ (n+1/2)\Delta t)}$$

where $\zeta_- = \zeta - h\ \Delta t/2$ for the first row and $\zeta_- = \zeta - \omega\ \Delta t/2$ for the other rows.

Step 6. and the following equality in the *y* direction at time $(n+1)\Delta t$

$$\begin{pmatrix} R_{y\pm}\\ u\\ \omega \end{pmatrix}_{(x,\ y,\zeta,(n+1)\Delta t)} = \begin{pmatrix} R_{y\pm}\\ u\\ \omega \end{pmatrix}_{(x,\ y_\pm,\zeta,\ (n+1/2)\Delta t)}$$

where $y_{\pm} = y - \left(\upsilon \pm \sqrt{gh}\right)\Delta t/2$ for the first row and $y_{\pm} = y - \upsilon\,\Delta t/2$ for the other rows.

Step 7. Finally, we can apply the following equality in the *x*- direction at time $(n+1)\Delta t$

$$\begin{pmatrix} R_{x\pm}\\ \upsilon\\ \omega \end{pmatrix}_{(x,\ y,\zeta,(n+1)\Delta t)} = \begin{pmatrix} R_{x\pm}\\ \upsilon\\ \omega \end{pmatrix}_{(x_\pm,\ y,\zeta,(n+1/2)\Delta t)}$$

where $x_{\pm} = x - \left(u \pm \sqrt{gh}\right)\Delta t/2$ for the first row and $x_{\pm} = x - u\,\Delta t/2$ for the other rows.

These seven steps will advance the solution of Eqs. (13) by one time-step Δt.

5. ALGORITHM FOR THE NUMERICAL SOLUTION OF THE ABOVE SYSTEM

1) divide the finite interval ($-a < x < a$) into equal subintervals Δx with finite number N equal to $2a/\Delta x$,
2) divide the finite interval ($-b < y < b$) into equal subintervals Δy with a finite number M equal to $2b/\Delta y$,
3) divide the finite interval ($-c < z < c$) into equal subintervals Δz with finite number K equal to $2c/\Delta z$,

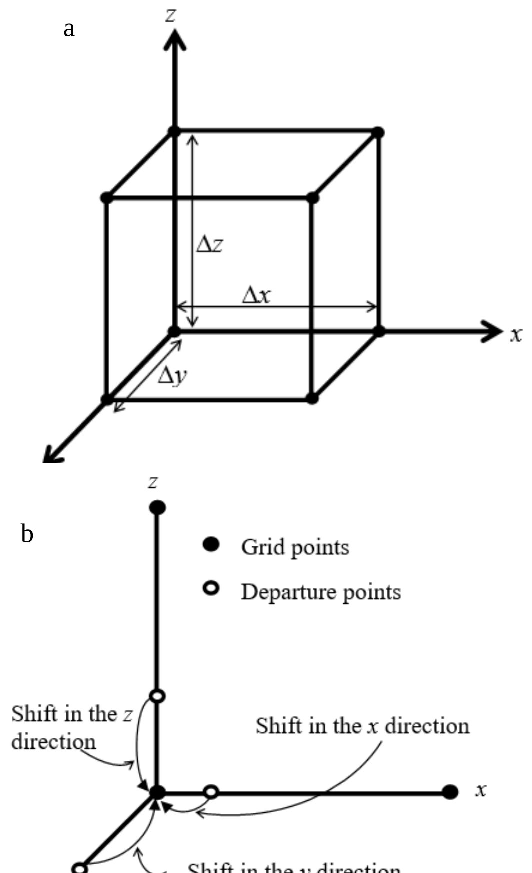

Fig.2 Modeling of the sphere grids (a) the dimension of the regular hexahedral grid (b) the grid and departure points.

4) a mesh of a regular hexahedral grid will be generated inside the spherical basin, Fig. (2a),
5) insert the discretized boundary and initial conditions at each grid point,
6) Start the entire cycle from step 1 to step 7 will advance the solution by one time step. to calculate the values of the functions at the point of departure,
7) the values of the functions at the grid points of the regular hexahedral can be calculated by shifting the values of the function at the departure points using a cubic spline interpolation, Fig. (2b),
8) Use the results of (7) as initial conditions to solve for the second time step.

6. RESULTS AND DISCUSSIONS

In this section, we give a numerical solution to the above problem, for some particular case of a spherical basin with radius equal to 1 m, the domain of the basin is covered with a uniform mesh of cubic grid size $0.01\text{ m} \times 0.01\text{ m} \times 0.01\text{ m}$ and a time step $\Delta t = 1$ sec. These calculations are effected with $200 \times 200 \times 200$ grid points. The level of water inside the basin is at 0.5 m from the bottom of the basin. The basin rotates around its z-axis with angular velocity Ω, The values of u, υ and ω are initially stationary but the value of the Coriolis parameter ($f = 2\Omega$) is used to start the evaluation of the free surface elevation. This is the forcing mechanism to make the water level start to flow. The shape of free surface elevation has been illustrated in Figs. 3 and 6 for different values of the Coriolis parameter f. It is found that the effect of the Coriolis parameter is decreasing with the elevation of the free surface and the velocity with the decrease of the value of f. Moreover, it is clear that due to the balance between the centrifugal and gravity forces, the free surface almost attains a parabolic shape.

Figures 4 and 5 illustrate the components of surface water velocity. In the animation of these pictures, we observe that a crown of velocity is constructed and moves from the center to circumference with the increasing of time. Generally, we observe that u (in x-direction), and υ (in y-direction) increase with the increase of time.

Figures 7-9 illustrate the effect of Coriolis parameter f on the three components of velocity: ω (in ζ -direction), u and υ, respectively. It is clear that the three components of the velocity increase with the increase of the parameter f. A typical profile of the vertical velocity " ω " against the vertical distance ζ, at different calculated Coriolis parameters f is illustrated in Fig. (7). It is noticed that the vertical velocity increases with the increase of the parameter f.

Figure (8) shows the horizontal velocity u for various values of Coriolis parameter f. It is found that the maximum point of velocity approaches to the center line of the sphere for a small values of f. This maximum point increases and moves away from the center line with the increasing of the Coriolis parameters.

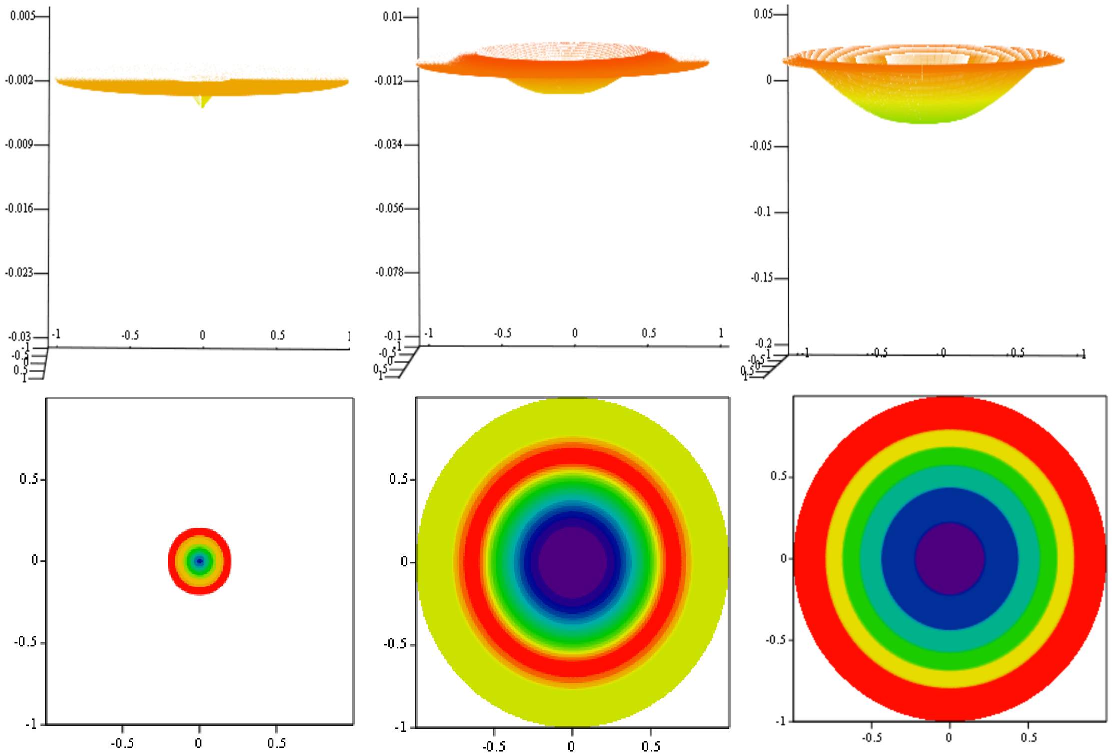

Fig.3 free surface elevation

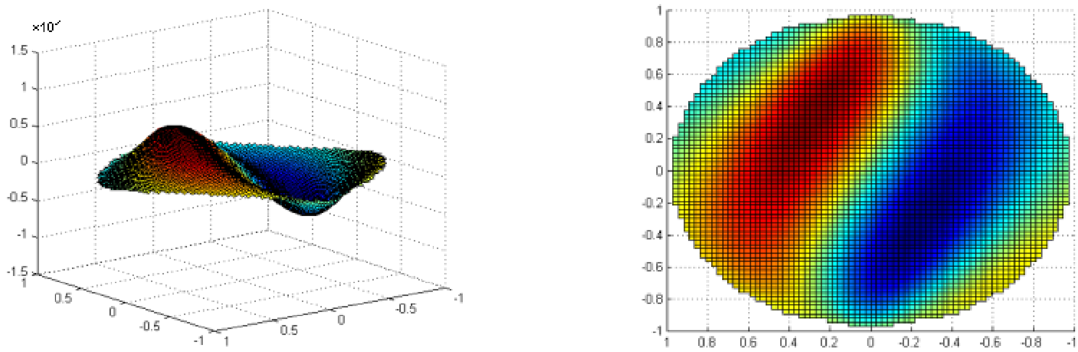

Fig.4a surface water velocity u (in x-direction) of the sphere which rotated under Coriolis parameter f = 0.2 at a time t = 200

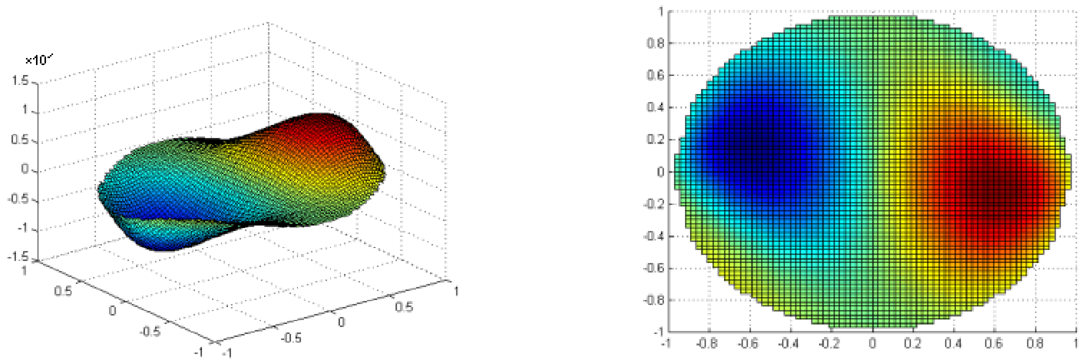

Fig.4b Surface water velocity u (in x-direction) of the sphere which rotated under Coriolis parameter f = 0.2 at a time t = 400

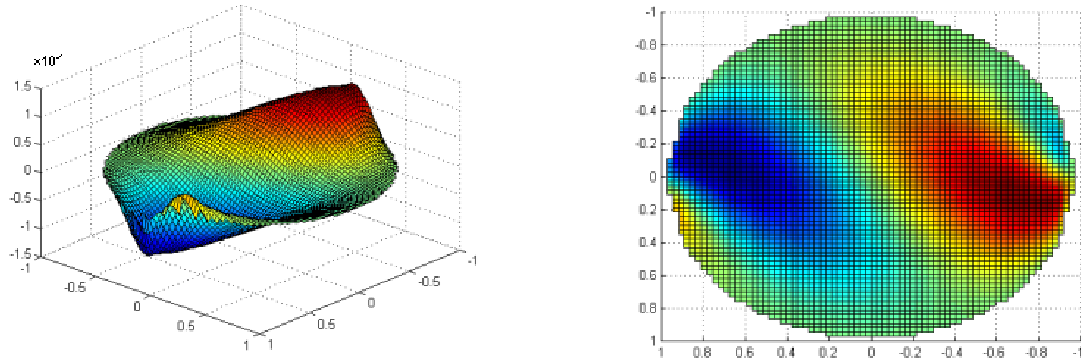

Fig.4c surface water velocity u (in x-direction) of the sphere which rotated under Coriolis parameter f = 0.2 at a time t = 800

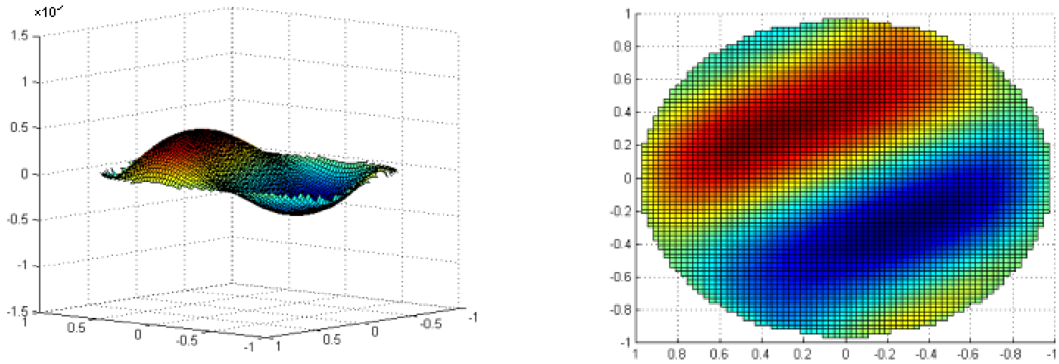

Fig.5a Surface water velocity υ (in y-direction) of the sphere which rotated under Coriolis parameter f = 0.2 at a time t = 200

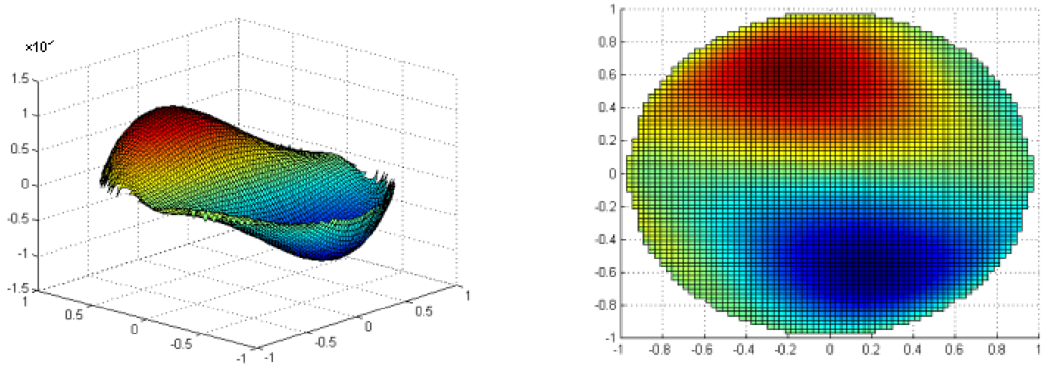

Fig.5b Surface water velocity υ (in y-direction) of the sphere which rotated under Coriolis parameter f = 0.2 at a time t = 400

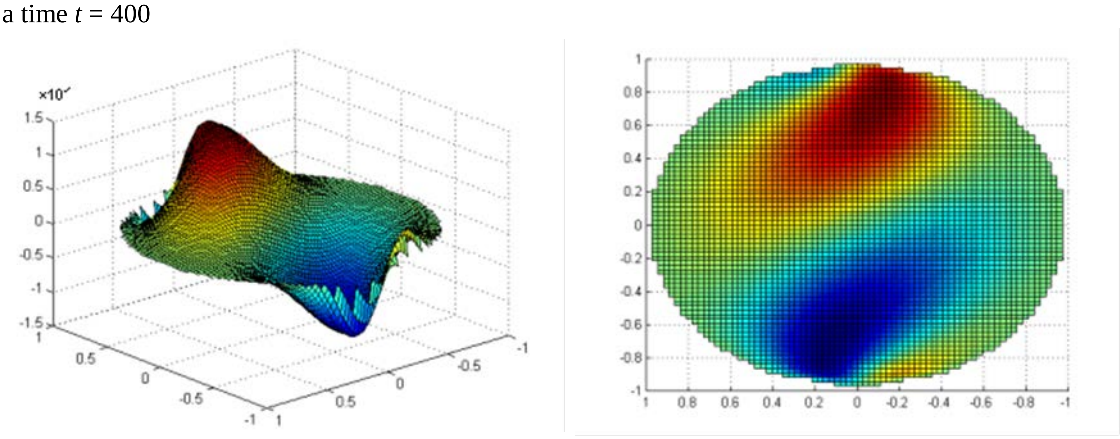

Fig.5c surface water velocity υ (in y-direction) of the sphere which rotated under Coriolis parameter f = 0.2 at a time t = 800

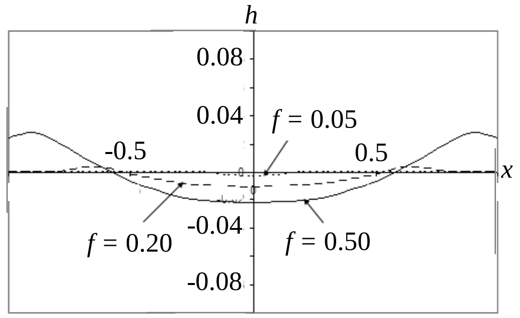

Fig.6 An elevation of the free surface

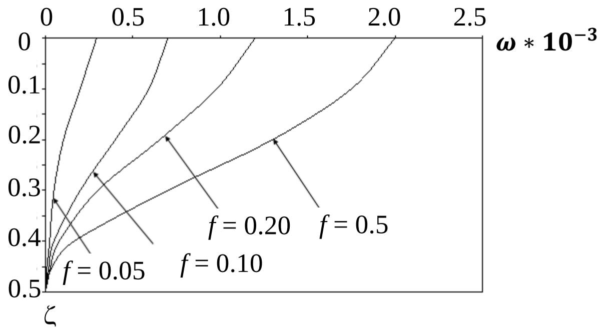

Fig.7 The velocity component in ζ direction with different Coriolis parameters at t = 400

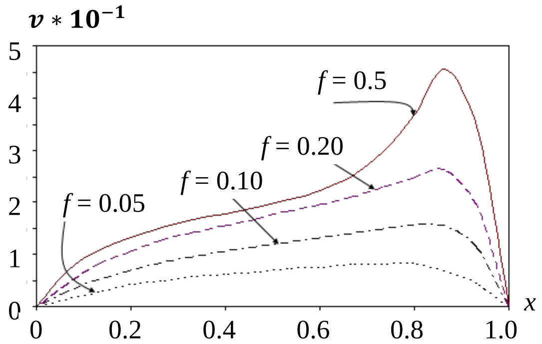

Fig.8 The velocity component in x direction with different Coriolis parameters at t = 400

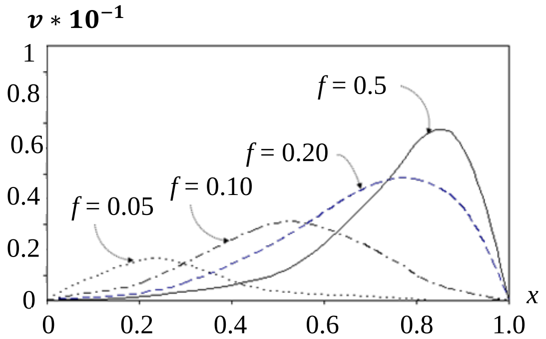

Fig.9 The velocity component in y direction with different Coriolis parameters at t = 200

Figure (9) shows the variation of horizontal velocity with distance x for various values of Coriolis parameter f. It is clear that starts from zero and overshoots to the maximum near the sphere surface and then decreases to zero.

7. CONCLUSION

We applied a fractional step method for the numerical solution of the three-dimensional nonlinear shallow water equation on a rotating spherical surface. The three-dimensional shallow water equations are split in three one-dimensional problems, each one in each dimension by using the Riemann invariants. The simplicity of the method makes it the method par excellence for computers of parallel architecture. The method is efficient [6,7,16] and has little numerical diffusion, since it evolves the equations without the iterative steps involved in the multidimensional interpolation problem. Therefore, the fractional step method has the advantage of reducing the multidimensional matrix problem into an equivalent one-dimensional problem. The absence of iterative steps and because the problem becomes one-dimensional in the present technique makes it very suitable for problems in which small time steps and grid sizes are required. We can decrease the time steps and grid sizes to increase the accuracy without any problem from the computer and without needing large ram, for instance, in this problem we want the computer occupied in its ram for the three one-dimensional matrices X, Y, Z as 200 + 200 + 200 = 600 cells but if we want to consist a three-dimensional matrices for X, Y, Z we need 200 × 200 × 200 = 8000000 cells in the ram. Increasing finer grids produces a mesh with too many elements and the multidimensional matrices thus becomes too large in size. Therefore, we become a need for a computer with a special specification, in addition there are increasing in the round-off and truncation errors. Moreover, the method provides numerical algorithms which are more efficient than other classical schemes. The velocity components for the rotating liquid inside the spherical basin are obtained. The numerical results showed that the free surface attains a parabolic shape, and this due to the balance between the centrifugal force and the gravity force. Moreover, it is found that the elevation of the free surface and the velocity components decrease with the decrease of the Coriolis parameter.

8. REFERENCES

[1] Rayleigh L., On the vibrations of rectangular sheet of rotating liquid, Phil. Mag. Vol. 5, 1903, pp.297–301.

[2] Greenspan H., The Theory of Rotating Fluids. Cambridge University Press, Cambridge, 1968.
[3] Magdalena I. & Wiryanto L. H., Wave generation on an inclined open channel with a bump. GEOMATE Journal, Vol. 19, Issue 76, 2020, pp. 126–133.
[4] Magdalena I., Suhardi J. L. E. & Adityawan M. B., Analytical and numerical studies for the reduction of wave run-up height by a submerged breakwater, GEOMATE Journal, Vol. 20 Issue 77, 2021, pp. 1–9.
[5] Yakimiw E., and Robert A., Accuracy and stability analysis of a fully implicit scheme for the shallow-water equations. Mon. Weather Rev. Vol. 114, Issue 1, 1986, pp.240-244.
[6] Shoucri M., The application of a fractional steps method for the numerical solution of the shallow water equations. Computer Physics Communications, Vol. 164, 2004, pp.396-401.
[7] Shoucri M., Numerical solution of the shallow water equations with a fractional step method. Computer Physics Communications, Vol. 176 Issue 1, 2007, pp.23-32.
[8] Muliati Y., Wurjanto R., Kelvin J., & Pranowo W., (2018). Application of swan model for hindcasting wave height in jepara coastal waters, north java, GEOMATE Journal, Vol. 15, Issue 48, pp. 114–120.
[9] Crandall M., and Majda A., The method of fractional steps of conservation laws, Numer. Math. Vol. 34, 1980, pp.285-314.
[10] Miura N., Nakamura D., Kawaguchi T., & Kawajiri, S., Investigation and stability analysis of slope failure at extremely shallow layer after snowmelt in snowy cold regions, GEOMATE Journal, Vol. 22, Issue 92, 2022, pp. 109–115.
[11] Yanenko N.N., The method of fractional steps; the solution of problems of mathematical physics in several variables. Springer-Verlag, Berlin, New York, 1971.
[12] Strang G., On the construction and comparison of difference schemes, SIAMJ. Numer. Anal., Vol. 5, 1968, pp.506-517.
[13] Abd-el-Malek M. B., and Helal M. M., Application of a fractional steps method for the numerical solution of the two-dimensional modeling of the Lake Mariut, Applied Mathematical Modelling Vol. 33, 2009, pp.822–834.
[14] Takeuchi J., Kawabata M., and Fujihara M., Numerical analysis on the occurrence of thermal convection in flowing shallow groundwater, International Journal of GEOMATE, Vol. 11, Issue 27, 2016, pp. 2688-2694
[15] Pohn E., M. Shoucri G., Kamelander, Eulerian Vlasov codes, Comp. Phys. Commun. Vol. 166, Issue 2, 2005, pp.81-93.
[16] Pohn E. M., Shoucri G., Kamelander, Study of the formation of a charge separation at a plasma edge. Part I. The numerical integration of a Vlasov equation possessing an invariant, Computer Physics Communication, 137, 380-395; Study of the formation of a charge separation at a plasma edge. Part II. Comparison between three different interpolation methods for the solution of the kinetic Vlasov equation, Computer Physics Communication, Vol.137, 2001, pp.396-404.
[17] Abd-el-Malek M. B., and Helal M. M., Application of a fractional step method for the numerical solution of the shallow water waves in a rotating rectangular basin, International Journal of Computer Mathematics, Vol. 87, Issue 10, 2010, pp.1–12.Awal ASMA, Hosseini H. and Hossain M.Z., Strength, Modulus of Elasticity and Shrinkage Behaviour of Concrete Containing Waste Carpet Fiber, International Journal of GEOMATE, Vol. 9, Issue 17, 2015, pp. 1441-1446.